

Numerical study of the out-of-equilibrium phase space of a mean-field spin glass model

Andrea Baldassarri*

*INFN, Sezione di Roma I Dipartimento di Fisica, Università "La Sapienza" Piazzale Aldo Moro, 00187 Roma, Italy
and CEA, Service de Physique de l'Etat Condense (SPEC) Orme des Merisiers, Gif sur Yvette 91191 Cedex, France*

(Received 29 May 1998)

We present a numerical study of the nonequilibrium dynamics of the Sherrington-Kirkpatrick model. We analyze the behavior of the system for different system sizes N and time scales t , in order to identify the correct out-of-equilibrium regime. We find evidence of aging behavior in the dynamics of the system, compatible with a weak-ergodicity breaking scenario. In addition, we obtain a pictorial characterization of the out-of-equilibrium phase space that presents some analogies with the hierarchy of states found in equilibrium.
[S1063-651X(98)03912-9]

PACS number(s): 05.70.Ln, 75.50.Lk, 02.70.Lq

I. INTRODUCTION

The past few years have witnessed an upsurging interest in the nonequilibrium properties of spin glasses [1–3]. Experiments have shown a very rich behavior in many different materials (see, for example, [4–6]) that is generically defined as the “aging phenomenon.” Simulations carried out for three-dimensional spin glass models [7] showed some of the characteristics (slow dynamics, aging) seen in experiments, but a complete theoretical interpretation of the phenomenon is still lacking. Recently, a theoretical analysis [8] of the nonequilibrium dynamics of mean-field models, such as the Sherrington-Kirkpatrick (SK) model [9], has contributed to shedding light on the issue. Despite the mean-field approximation, the SK model shows a rich nonequilibrium behavior that is still not completely understood. In particular, it will be interesting to have a clear picture of the phase space in which the model evolves, in order to connect its behavior with recently proposed phenomenological descriptions of aging phenomena [10].

Here we present a numerical study of the out-of-equilibrium dynamics of the SK model, in order to obtain a description of the phase space. We find two clearly distinct dynamical regimes: a genuine out-of-equilibrium regime that will be dominant in the thermodynamic limit followed by an intermediate regime that is solely due to the finite system size. The second regime corresponds to the approach to equilibrium of a finite system. This result is based on the analysis of the dynamical behavior of the mean-square value of the overlap between two replicas, which is commonly employed in simulations to determine the equilibration of the system [11–13].

Once these regimes are clearly identified, we focus our analysis on the first regime, which is the one described theoretically [8]. We find that the behavior of the system is consistent with the “weak-ergodicity breaking scenario” proposed by Bouchaud [10,14]. In this scenario, the system is not confined in a finite region of the phase space and wanders indefinitely in search of the equilibrium state. A clear

picture of this behavior is obtained by studying the two-times autocorrelation functions.

The phase space visited by the system displays an interesting self-similar landscape, which is reminiscent of the hierarchical structure found for the *equilibrium* phase space of the model [1]. In addition, in order to obtain a pictorial view of the dynamics of the system, we use the *dynamics clonation* technique recently introduced [15–18]. In this way, we show evidence that the system evolves through “valleys” and “canyons,” rather than jumping between independent “traps.”

This paper is organized as follows. In Sec. II we present the model and we discuss some general considerations regarding different limiting procedures leading to equilibrium or nonequilibrium dynamics. Here we define what we mean for out-of-equilibrium dynamics. Section III is devoted to the numerical results. At first (Sec. III A) we present a quantity that we use for the determination of the equilibrium of the system. By studying its scaling behavior with the size of the system, we find two different dynamical nonequilibrium regimes. The scaling of the crossover time between the two regimes helps us to identify the first one as the authentic relevant regime for the out-of-equilibrium dynamics. In Sec. III B we focus on this *out-of-equilibrium regime*. Measuring the autocorrelation functions we find generic aging properties and a scenario compatible with a *weak-ergodicity breaking*. The energy density of the system and the staggered magnetization give further support to the analytical predictions of [8,19]. In Sec. III C we present the procedure of dynamics clonation [15–18] and report some results obtained with it. Our conclusions are given in Sec. IV.

II. GENERAL CONSIDERATIONS

In the present work we study the Monte Carlo dynamics (with the Metropolis sequential updating algorithm) of the SK model [9], defined by the Hamiltonian

$$H_J[\sigma] = -\frac{1}{2} \sum_{i \neq j} J_{ij} \sigma_i \sigma_j. \quad (1)$$

The J_{ij} are random variables with variance $1/\sqrt{N}$, where N is the total number of spins (or size of the system).

*Electronic address: andreab@spec.saclay.cea.fr

It is well known [1] that the SK model (1) undergoes a phase transition at $T_c=1$. The order parameter is the Parisi $q(x)$ function that is related to the overlap distribution function of the equilibrium states $P(q)$: $P(q) = (dq/dx)^{-1}$ (for a recent numerical analysis, see [20]). To monitor the order parameter, $q(x)$, we measure the first nonzero momentum of the $P(q)$ overlap distribution, which, in the zero field case, is the second momentum. In the simulation, it corresponds to

$$q_2(N,t) = \left\langle \left[(1/N) \sum_{i=1,N} \sigma_i(t) \tau_i(t) \right]^2 \right\rangle. \quad (2)$$

Here $\sigma_i(t)$ and $\tau_i(t)$ denote the configuration at time t of two realizations of the dynamics (J_{ij} fixed), with independent randomly chosen initial configurations and independent noise realization. (Hereafter we shall call them *replicas*.) We follow the standard notation, indicating the thermal average (different noise realization, but fixed J_{ij}) with $\langle \dots \rangle$, and the sample average (different chosen J_{ij}) with $\overline{\dots}$. In the present work we always used at least 10 noise realizations and 200 different samples (unless otherwise mentioned).

Let us observe that, obviously, during a simulation any measured quantity O always depends on the size of the system (the number of spins N) and on time (the number of Monte Carlo sweeps preceding the measuring time t). The equilibrium value is given by the *asymptotic limit* (AL) $\lim_{t \rightarrow \infty} O(N,t) = O(N)$. The thermodynamical analytical calculations give the equilibrium value for an infinite system, that is, the *thermodynamical limit* (TL) of the equilibrium quantity: $\lim_{N \rightarrow \infty} O(N) = O_{\text{eq}}$. So, if we are interested in the equilibrium properties of the system, we have to consider TL after AL for the measured quantity. On the contrary, the reverted limiting procedure (AL after TL) may give very different results, especially if the system undergoes a phase transition, that is, an ergodicity breaking due to the TL. Some recent analytical works [21,8] deal with this opposite ordered limit procedure to describe the out-of-equilibrium properties of spin glasses. We call the asymptotic dynamics of an infinite system, in the sense of this order of limits (AL after TL), the *out-of-equilibrium dynamics*.

In a computer simulation, we cannot perform either AL or TL. We consider systems of growing sizes, and for each one we consider a time after which the system is equilibrated. The correct criterion for choosing such equilibration time is not so trivial, especially for systems like spin glasses, which evolve extremely slowly as shown clearly by experiments. We can consider the simulated spin glass equilibrated when the two-times quantities (2TQ) do not depend explicitly upon both times, but only upon the time difference [time translational invariance (TTI)]. (We expect that this is enough for a mean-field model.) For example, if we consider the two-times autocorrelation function

$$C_N(t,t') = \left\langle \frac{1}{N} \sum_{i=1,N} \sigma_i(t) \sigma_i(t') \right\rangle \quad (3)$$

we are sure that the system forgot the initial ($t=0$) randomly chosen configuration only for the TTI: $C_N(t,t') = C_N(t-t')$. Unfortunately, the measurements of 2TQ are very computer time consuming. It would then be better to use an

equilibration criterion involving only one-time quantities (1TQ). A typical (1TQ), for example, is the energy density of the system at time t :

$$E(N,t) = (1/N) \overline{H(t)}. \quad (4)$$

However, in a glassy system, a 1TQ may reach an asymptotic value, very close to or equal to its equilibrium value, even when the system is very far from equilibrium, i.e., the autocorrelation function (3) is far from being homogeneous in times. (In this work we try to show that this happens for the energy density of the SK model.) Consequently, checking for the asymptotic value of a 1TQ only can lead to erroneous results.

III. NUMERICAL SIMULATIONS

A. The overlap as a criterion for equilibration

The quantity q_2 (2) is often used to determine the equilibration of the SK model (for more subtle equilibration criteria, see [13]). For example, the identity $q_2 = 1 - 2TE$ [12] is used in [11] to determine the times $t < t_0$ to skip before collecting the equilibrium measure. (E is the equilibrium value of the energy density (4): $E = \lim_{N \rightarrow \infty} \lim_{t \rightarrow \infty} [E(N,t)/N]$).

On the contrary, in this work, we are interested in the *dynamical evolution before equilibration*.

We check explicitly the hypothesis that measuring q_2 represents a good criterion for equilibration, as shown in Fig. 1, where we confront the measures of q_2 and of the autocorrelation functions (3).

We concentrate much of our efforts studying q_2 before it reaches the equilibrium value and in particular its scaling behavior with respect to the size of the system.

We simulate the dynamics of $q_2(N,t)$ for several system sizes at fixed temperature. The value of $q_2(N,t=0)$ is generally $1/N$, because the starting configuration for each replica is chosen randomly and independently. A different choice for the starting value of q_2 is not determinant for the subsequent dynamics, apart from the very first steps.

The dynamics of $q_2(N,t)$ is characterized by a monotonic growth (on a logarithmic time scale) up to its equilibrium value. We identify two nonequilibrium regimes, characterized by different scaling properties with respect to the size of the system.

(i) *Out-of-equilibrium regime*. In the first regime, $q_2(N,t)$ scales as $1/N$, with the law

$$q_2(N,t) \propto (1/N) \ln(t).$$

In Fig. 2 we show the (size-independent) quantity $Nq_2(N,t)$ versus t for systems of different size. (The temperature dependence is restricted to the proportionality constant.)

(ii) *Intermediate regime*. As the $q_2(N,t)$ reaches a fraction of its equilibrium value, the scaling behavior changes. Figure 3 shows the departure of the $Nq_2(N,t)$ from the ‘‘universal’’ (that is, large N) curve for systems of different sizes.

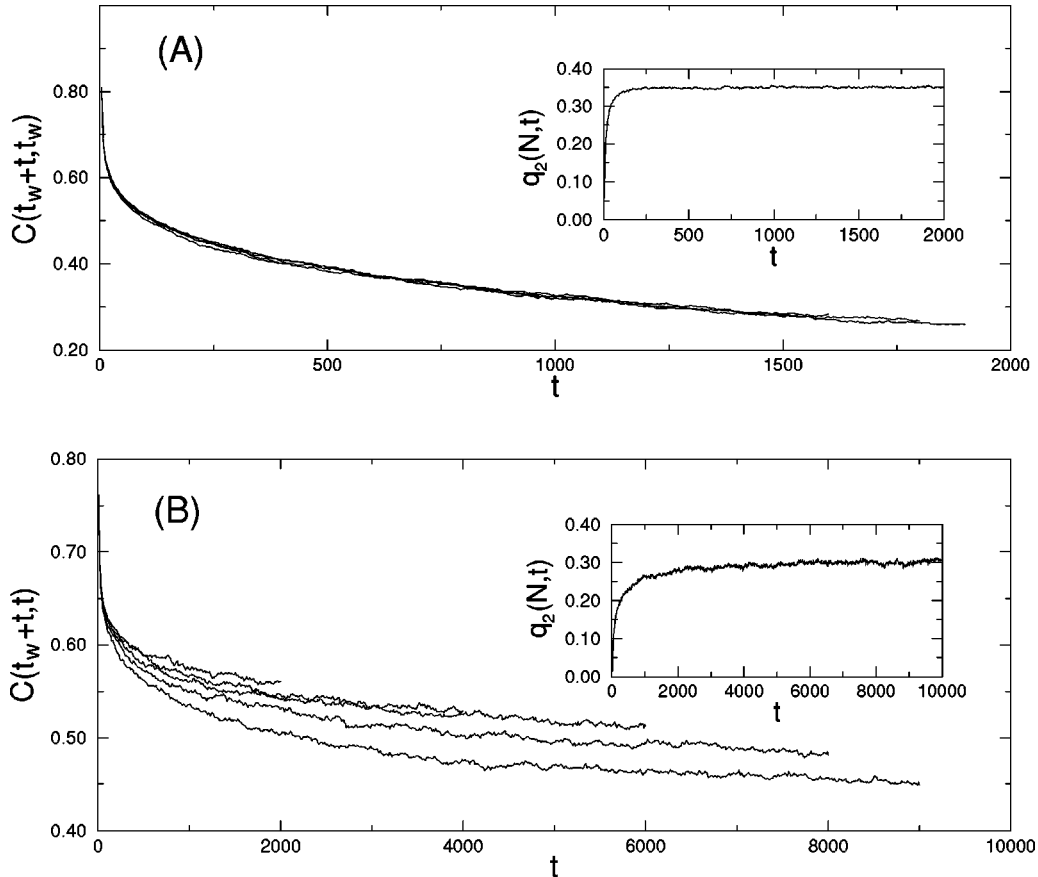


FIG. 1. The autocorrelation functions (3) become time-homogeneous only when $q_2(N, t)$ (in the insets) reaches its equilibrium value. In (a) the system (64 spins) is equilibrated ($T=0.5T_c$) as shown by the independence of the autocorrelation functions $C(t_w+t, t_w)$ by t_w ($t_w = 100, 200, 400, 800, \text{ and } 1600$ Monte Carlo sweeps). In the inset, $q_2(N, t)$ has reached its equilibrium value. In (b) the system (480 spins, $T=0.5T_c$) is out-of-equilibrium. The autocorrelation functions show a strong dependence of t_w (from bottom to top, $t_w = 1000, 2000, 4000, 6000, 8000$). In the inset the equilibrium value of $q_2(N, t)$ is greater than 0.3 for the chosen temperature $T=0.5T_c$. The data refer to 200 different samples (i.e., 200 different chosen $\{J_{i,j}\}$). For each sample we use at least 10 replicas (see text) to measure $q_2(N, t)$.

We tried a fit for this scaling. Here we simply mention that, qualitatively, we get a $1/N^\alpha$ scaling (with α temperature dependent, ranging from 1 to 1/3). We called this new scaling regime the *intermediate regime*. Let us note here that the $q_2(N, t)$ is a highly non-self-averaging quantity, and the sample-to-sample fluctuations are strong. So a plausible interpretation for the intermediate regime behavior is that some of the simulated replicas reach equilibrium during this regime and the others do not. In this sense we think of this regime as a transient between the well defined out-of-equilibrium regime and the equilibrium dynamics of the system.

The crossover between the two regimes is shown in the inset of Fig. 3. We define the crossover time t_{co} as the time before the difference between the $Nq_2(N, t)$, and the universal curve $\lim_{N \rightarrow \infty} Nq_2(N, t)$ reaches a fixed tolerance value. We believe this is a linear behavior.

Let us note here that an infinite sized system, started from a random configuration (i.e., physically, a system after an infinitely fast quench from very high temperature or magnetic field), will always stay in the first out-of-equilibrium regime. The value of $q_2(t) = \lim_{N \rightarrow \infty} q_2(N, t)$ would be identically zero, indicating that each replica is orthogonal (zero

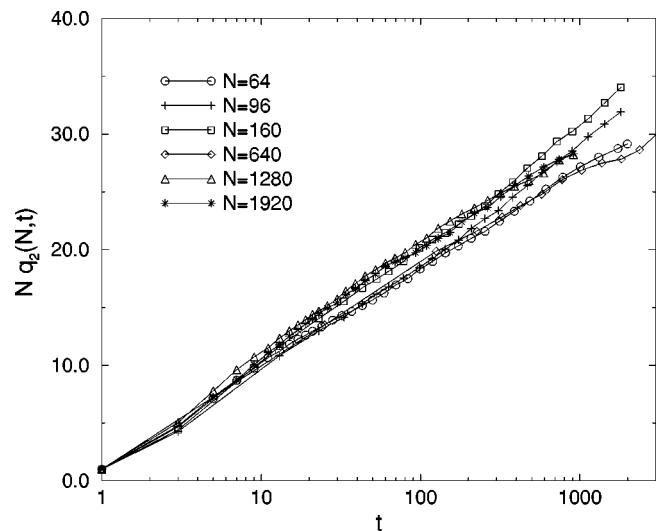


FIG. 2. $q_2(N, t)$ in the out-of-equilibrium regime multiplied by N for systems of different sizes ($N=64, 96, 160, 640, 1280, \text{ and } 1920$ spins). For the chosen temperature ($T=0.2T_c$) the curves seem to collapse in the simulated time window ($t < 2000$ Monte Carlo sweeps). The data refer to a minimum of 10 replicas for each of the 200 samples.

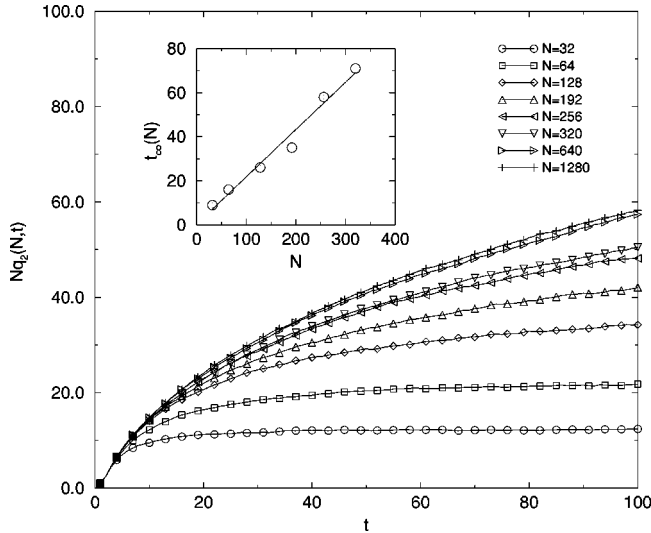


FIG. 3. Crossover from the out-of-equilibrium regime to the intermediate regime. The plot represents the quantity $Nq_2(N,t)$ vs t for several systems of growing size ($N = 32, 64, 128, 192, 256, 320, 640,$ and 1280 spins) evolving at $T = 0.5T_c$. Note that the curves associated to $N = 640$ and $N = 1280$ collapse, indicating that the two systems are still both in the out-of-equilibrium regime for the whole time window ($t < 100$ Monte Carlo sweeps). The curve for $N = 1280$ has been used as the limiting curve for the determination of the crossover time (t_{co}). For these curves we have used 1000 samples. In the inset the cross-over time (t_{co}) is displayed as a function of N with a tentative linear fit.

scalar product of the vector configurations) with respect to the other. It means that each replica visits a different mutually orthogonal sector of the phase space.

B. Out-of-equilibrium regime

As we are interested in the out-of-equilibrium dynamics of the model, in the sense of the ordered limit procedure AL after TL, we study the dynamics of some quantities in the first dynamical regime, i.e., the out-of-equilibrium regime.

The autocorrelation function (3) shows aging behavior (see Fig. 4), compatible with the weak-ergodicity breaking hypothesis [10].

We cannot exclude a nonzero asymptotic value of the autocorrelation functions, but as we do not see evidence of this in our simulated time windows, we will assume in the discussions a true weak-ergodicity breaking scenario.

Remarkably enough, if we plot the autocorrelation function $C(t_w + \tau, t_w)$ versus τ/t_w , they do not collapse (there is not a simple τ/t_w law), but all cross at a certain value.

The relaxational dynamics of the energy density for the SK model has been extensively studied (for example in [22]). Here we want to focus on its asymptotic value. To this aim, we reparametrize the energy density curve with respect to the overlap q_2 , which serves here as a dynamical “clock,” indicating the equilibration stage of the system at time t .

Figure 5 shows the result of such reparametrization. The line is the equilibrium relation $E = -\beta/2(1 - q_2)$. The first two curves refer to systems that reach equilibrium at the end of the simulation. The others, with growing size, are farther

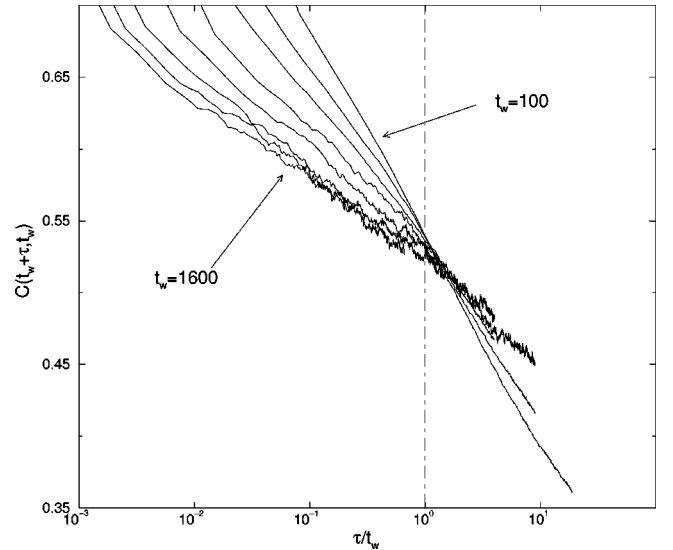


FIG. 4. Autocorrelation functions $C(t_w + \tau, t_w)$ vs τ/t_w for different t_w ($t_w = 100, 200, 400, 800, 1000, 1200, 1400,$ and 1600 Monte Carlo sweeps). The data refer to a system of $N = 640$ spins evolving at $T = 0.5T_c$.

from equilibrium, but closer to the energy density equilibrium value.

A plausible proposal for the limiting curve associated with an infinite system is a step function that, starting from $E = 0, q_2 = 0$, abruptly collapses to the constant value E

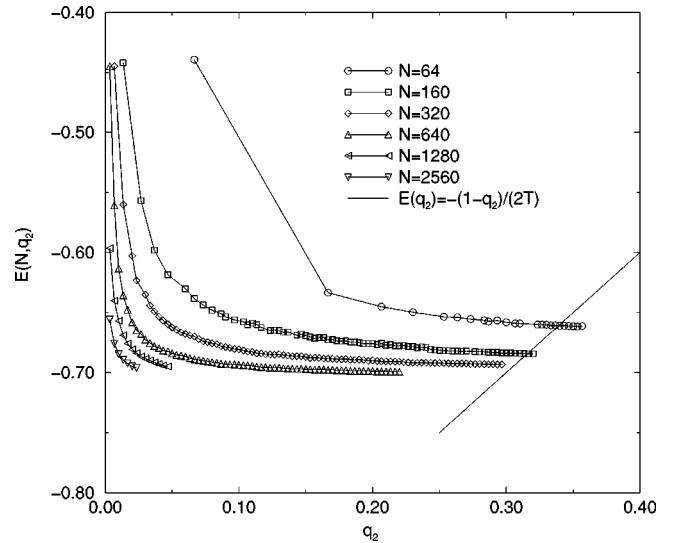


FIG. 5. Energy density $E(N,t)$ versus the corresponding value of $q_2(N,t)$ (time becoming a parameter). From top to bottom, the curves refer to growing-sized systems ($N = 64, 160, 320, 640, 1280, 2560$) evolving at the same temperature $T = 0.5T_c$. The first two curves (smaller systems) achieved equilibrium in the simulated time range; the remaining curves refer to systems that did not achieve the equilibrium. The relation shown as a straight line [indicating the equilibrium value for $E(N,t)$ and $q_2(N,t)$] is correct for any size with a Gaussian coupling distribution. In our simulation we do not expect a strict validity of the relation for finite-sized systems, because we use for the couplings J_{ij} a two-value $\{-1; 1\}$ distribution. Moreover, we have larger errors on the abscissa values, due to the lack of self-averageness of $q_2(N,t)$ (large sample-to-sample fluctuations).

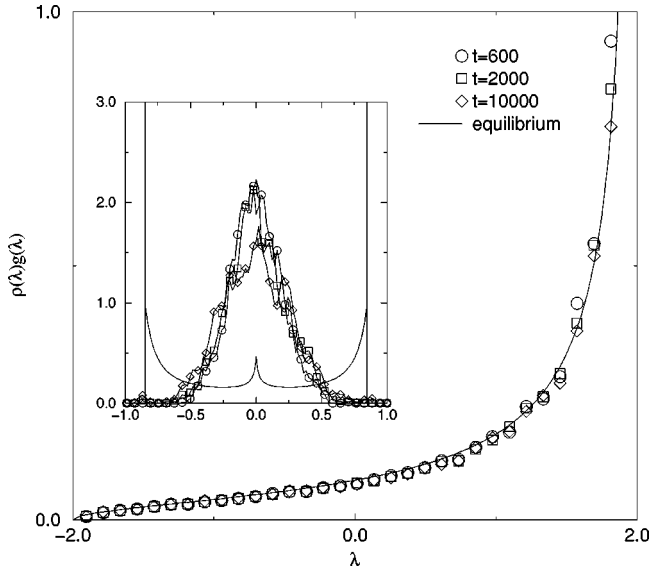


FIG. 6. Staggered magnetization calculated at different nonequilibrium times (figure from Ref. [19]). The data refer to a system size of $N=992$ spins evolving at $T=0.3T_c$ for different times ($t=600$, 2000, and 1000 Monte Carlo sweeps). The full lines correspond to the prediction of the Parisi mean-field theory for the equilibrium. In the inset we show the overlap distribution for the same times, while the full line is a sketch of the theoretical (Parisi) $P(q)$. Due to the self-averageness of the staggered magnetization, we use here a very small number of samples, allowing for larger times.

$=E_{\text{eq}}$ for $q_2 > 0$. Besides, it means that this 1TQ does not represent a good choice for the determination of the equilibration time. To corroborate such a result, we summarize here previously published results [19].

Consider σ_λ the projection of the configuration vector $\vec{\sigma}(t) = \{\sigma_i(t)\}$ on the set of eigenvectors $\vec{J}(\lambda)$ of the coupling matrix $\{J_{ij}\}$. We measure the so-called staggered magnetization, i.e., $g_{N,t}(\lambda) = \overline{\langle [\sigma_\lambda(t)]^2 \rangle}$, where $\sigma_\lambda(t) = \sum_{i=1,N} \lambda_i \sigma_i(t)$, $\{\lambda_i\}$ being the coordinates of the $\hat{\lambda}$ eigenvector of the coupling matrix ($\sum_{j=1,N} J_{ij} \lambda_j = \hat{\lambda} \lambda_i$).

The staggered magnetization is a distribution that contains a lot of information. In particular, its first momentum is the energy density (4). More precisely, $\lim_{N \rightarrow \infty} E(N,t) = -\lim_{N \rightarrow \infty} \int_{-2}^2 \lambda \rho(\lambda) g_{N,t}(\lambda) d\lambda$, where $\rho(\lambda)$ is the well-known semicircle distribution for the eigenvalue of the J_{ij} random matrix [23].

In Fig. 6 we show the staggered magnetization, multiplied by the eigenvalue semicircle distribution $\rho(\lambda)$, compared with the equilibrium curve [24]. We note a very fast convergence of the out-of-equilibrium staggered magnetization to the equilibrium curve, when the system is still very far from equilibrium [as revealed by the $P(N,t;q)$ shown in the figure inset].

From the measure of the autocorrelation functions, the energy density, and the staggered magnetization, we get further insight into the geometrical nature of phase space visited from the system out-of-equilibrium. First, the weak-ergodicity breaking conditions [10] indicate that the system always escapes from the visited region (even if more and more slowly), i.e., waiting long enough that its configuration becomes orthogonal with the ancient one (zero autocorrela-

tion). The measures of the energy density and of the staggered magnetization allow a comparison between the phase space visited in the out-of-equilibrium and the equilibrium phase space (i.e., the configuration relevant in the Gibbs average). The out-of-equilibrium energy density seems to be equal to the equilibrium one, and (a stronger condition) the distribution of the projection of the out-of-equilibrium configurations with the eigenvectors of the J_{ij} coupling matrix is the same as in equilibrium. It seems to show a geometrical self-similarity of the phase space.

The existence and the meaning of a strict relation between non-equilibrium dynamics and equilibrium properties of spin glasses is a very interesting but still open problem, that stimulated many recent works [25,26]. The difficulties in the physical comprehension derive usually by the fact that very different quantities seems to be related (fluctuation dissipation ratio and equilibrium replicas overlap distribution). In this case, the relation between statics and dynamics is based on the same quantity, the staggered magnetization, that has the same simple geometrical interpretation in statics and dynamics (and the same self-averaging properties).

Our results for the energy density disagree with those of Scharnagl *et al.* in [27]. The results of their power-law fit on the first 130 steps for the energy dynamics of an infinite system (they use an interesting new procedure to simulate the dynamics of infinite-sized systems [28]) indicate an asymptotic energy value e_∞ different from the equilibrium value for temperature below $0.5T_c$. The numerical method implemented is based on the parallel dynamics of the Little model: $H_J[\sigma] = -\frac{1}{2} \sum_{i \neq j} J_{ij} \sigma_i \tau_j$, where the σ and the τ are independent degrees of freedom. It can be seen as a generalized SK model [that is recovered imposing a constraint ($\sigma_i = \tau_i$) on the degrees of freedom] or as a very special diluted SK model. The thermodynamics (equilibrium) of such a model has been shown [29] to be equivalent to the SK one (except if a first-order phase transition occurs [30]). Further investigation, and an explicit comparison between the non-equilibrium dynamics of the two models, may be needed.

C. Clonation procedure

To obtain a clearer picture of the geometrical landscape where the out-of-equilibrium dynamics takes place, we perform a particular simulation procedure that we call ‘‘clonation’’ [15–18]. Since we are interested in the phase-space region visited by the dynamics after a certain time t_w , we proceed to let a single system evolve with the usual Monte Carlo dynamics until such a time. At t_w we create a number of copies of this system, i.e., systems exactly in the same configuration (we *clone* it). Subsequently we let them (the original and the clones) evolve independently, that is to say with the same Hamiltonian, but different noise realizations.

There is a difference between these copies (clones) of the system and the previously defined *replicas*. The *replicas* start at time $t=0$ from *independently chosen configurations* and evolve with independent dynamics (same Hamiltonian, different noises), being, in this way, completely independent systems.

This *clonation* procedure is different from a damage-spreading procedure (see, for example, [31,32]), where two systems starting at a measured distance evolve with the same

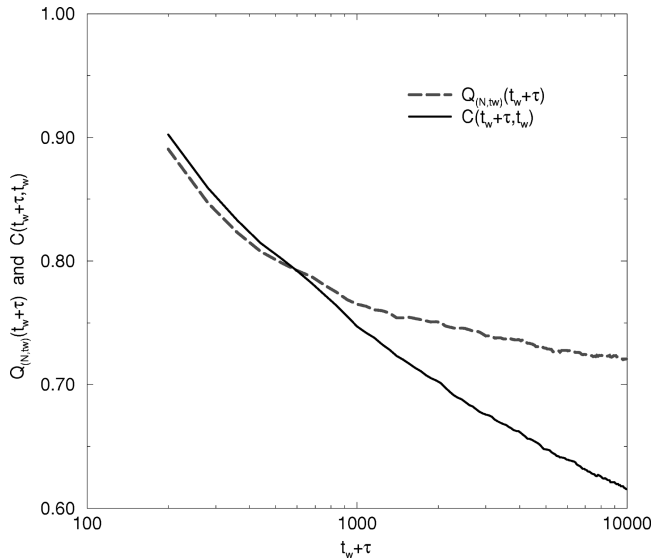


FIG. 7. Clonation of a system of $N=320$ spins at the time t_w = 100 Monte Carlo sweeps ($T=0.2T_c$). The plot shows the auto-correlation (3) and the clone-correlation (5) functions.

noise. The damage-spreading procedure was used to individuate transition temperatures which could be compared with equilibrium and dynamical transition temperatures.

Our aim here is to investigate the geometry of the phase space monitoring the autocorrelation function (3), and the *Clones-Correlation Function*, defined by

$$Q_{(N,t_w)}(t) = \left\langle \frac{1}{N} \sum_{i=1,N} (\sigma_i(t) \tau_i(t)) \right\rangle \quad (5)$$

(σ and τ are the spins of two different clones).

These quantities are simply related to the Euclidean distance in phase space. The autocorrelation (3) is related to the Euclidean distance between the configuration of the clones at the time t_w (the same for them all) with its own configuration at the time $t > t_w$ as $d_C = \langle (1/N) \sum_{i=1,N} [\sigma_i(t_w) - \sigma_i(t)]^2 \rangle = 2[1 - C_N(t, t_w)]$. Similarly, the clones correlation (5) is related to the distance between the clones (generated at the time t_w) at the time t : $d_Q = \langle (1/N) \sum_{i=1,N} [\sigma_i(t) - \tau_i(t)]^2 \rangle = 2[1 - Q_{(N,t_w)}(t)]$.

In Fig. 7 we show the results of the measurement. We see that at first we have $C > Q$, but, after some time of the order of t_w , this relation inverts, and we have $Q > C$.

(In the present work we do not get the asymptotic limit of Q . Due to the very slow relaxation of Q , we suspect that it goes to zero, but we cannot exclude a constant asymptotic value different from zero and the issue remains open [17,18].)

Remembering the relations of these quantities with the Euclidean distances, it means that at first the clones go away from each other more than the distance they drift away from the initial configuration at the time t_w . But afterwards, they continue their drift standing close and forgetting the initial t_w configuration. The simplest picture representing such a behavior is that of a dynamics following canyons or corridors: at first the clones span the width of the channel and, afterwards, they drift away along it.

If the situation were that of a series of independent traps (as, for example, in [10]), we would have seen a different behavior, probably with $Q = C$ at long times. Here, we see, at least, a kind of hierarchy of traps [14].

IV. CONCLUSIONS

The nonequilibrium dynamics of the SK model displays characteristic time scales that grow with the size of the system.

In the case of a large system, starting from a random configuration, which is equivalent to cooling the system abruptly from the high-temperature phase to the glassy phase, the dominant regime is the out-of-equilibrium regime [during which the $q_2(N,t)$ scales to zero as $1/N$]. In this situation the dynamics is nonstationary, presenting generic aging properties compatible with the scenario of weak-ergodicity breaking. As claimed by recent analytical works [21,8,19,26], the asymptotic configurations reached by an infinite SK model present some similarities with the equilibrium phase space: the out-of-equilibrium staggered magnetization is equal to the equilibrium one, as is the energy density [19]. However, the configurations visited by the system are not real equilibrium configurations and the system always escapes from them, never to return. These configurations present a sort of hierarchical structure. A clonation procedure shows that the dynamics takes place following corridors or canyons. The phase space looks like an almost flat labyrinth that the system explores more and more slowly, looking for equilibrium. This numerical procedure reveals that the spin-glass dynamics, even in the mean-field case, explores a complicated phase space, which cannot simply be thought of as a series of barriers and wells (see, for example, [33–35]). The problems of the characteristic width of the “canyons” [17] (related to the asymptotic value of the clone correlation) or the deep meaning of the “self-similarity” with equilibrium are still open.

ACKNOWLEDGMENTS

We thank L. F. Cugliandolo and J. Kurchan for their collaboration, and G. Parisi for the helpful supervision, throughout the development of this work. We are indebted to F. Ritort, R. Monasson, and S. Zapperi for their careful reading of the manuscript.

- [1] M. Mezard, G. Parisi, and M. A. Virasoro, *Spin Glass Theory and Beyond* (World Scientific, Singapore, 1986).
- [2] K. Binder and A.P. Young, *Rev. Mod. Phys.* **58**, 801 (1986).
- [3] K.H. Fischer and J.A. Hertz, *Spin Glasses* (Cambridge University Press, Cambridge, 1991).
- [4] L. Lundgren, in *Relaxation in Complex Systems and Related*

Topics, edited by I. A. Campbell and C. Giovannella (Plenum, New York, 1990).

- [5] E. Vincent, J. Hamman, and M. Ocio, in *Recent Progress in Random Magnets*, edited by D. H. Ryan (World Scientific, Singapore, 1987).
- [6] E. Vincent, J. Hamman, M. Ocio, J. P. Bouchaud, and L. F.

- Cugliandolo, in *Complex Behaviour in Glassy Systems*, edited by M. Rubi (Springer-Verlag, Berlin, in press).
- [7] H. Rieger, in *Annual Reviews of Computational Physics*, edited by D. Stauffer (World Scientific, Singapore, 1995), Vol. II.
- [8] L. F. Cugliandolo and J. Kurchan, *J. Phys. A* **27**, 5749 (1994).
- [9] D. Sherrington and S. Kirkpatrick, *Phys. Rev. Lett.* **35**, 1792 (1975).
- [10] J. P. Bouchaud, *J. Phys. I* **2**, 1705 (1992).
- [11] N. D. Mackenzie and A. P. Young, *J. Phys. C* **16**, 5321 (1983).
- [12] A. J. Bray and M. A. More, *J. Phys. C* **13**, 419 (1980).
- [13] R.N. Bhatt and A.P. Young, *J. Phys.: Condens. Matter* **1**, 2997 (1989).
- [14] J. P. Bouchaud and D. S. Dean, *J. Phys. I* **5**, 265 (1995).
- [15] Andrea Baldassarri, thesis, Università Degli Studi di Roma "La Sapienza," 1995 (unpublished).
- [16] L. F. Cugliandolo and D. S. Dean, *J. Phys. A* **28**, 4213 (1995).
- [17] A. Barrat, R. Burioni, and M. Mezard, *J. Phys. A* **29**, 1311 (1996).
- [18] Hajime Takayama, Hajime Yoshino, and Koji Hukushima, *J. Phys. A* **30**, 3891 (1997).
- [19] A. Baldassarri, L. F. Cugliandolo, J. Kurchan, and G. Parisi, *J. Phys. A* **28**, 1831 (1995).
- [20] M. Picco and F. Ritort, *J. Phys. I* **4**, 1819 (1994).
- [21] L. F. Cugliandolo and J. Kurchan, *Phys. Rev. Lett.* **71**, 173 (1993).
- [22] W. Kinzel, *Phys. Rev. B* **33**, 7 (1986); E. Marinari, G. Parisi, and D. Rossetti, *Eur. Phys. J. B* **2**, 495 (1998).
- [23] M. L. Mehta, *Random Matrices and the Statistical Theory of Energy Levels* (Academic, New York, 1967).
- [24] M. Mezard and G. Parisi, *J. Phys. (France) Lett.* **45**, L-707 (1984).
- [25] Enzo Marinari, Giorgio Parisi, Federico Ricci-Tersenghi, and Juan J. Ruiz-Lorenzo, *J. Phys. A* **31**, 2611 (1998).
- [26] Silvio Franz, Marc Mézard, Giorgio Parisi, and Luca Peliti, e-print cond-mat/9803108.
- [27] Andrea Scharnagl, Manfred Opper, and Wolfgang Kinzel, *J. Phys. A* **28**, 5721 (1995).
- [28] H. Eissfeller and M. Opper, *Phys. Rev. Lett.* **68**, 2094 (1992).
- [29] R. Brunetti, G. Parisi, F. Ritort, *Phys. Rev. B* **46**, 5339 (1992).
- [30] G. Parisi (private communication).
- [31] B. Derrida, *Phys. Rep.* **184**, 207 (1989).
- [32] I.A. Campbell and L. de Arcangelis, *Physica A* **178**, 29 (1991).
- [33] J. Kurchan and Laurent Laloux, *J. Phys. A* **29**, 1929 (1996).
- [34] F. Ritort, *Phys. Rev. Lett.* **75**, 1190 (1995).
- [35] Hajime Yoshino, *J. Phys. A* **30**, 1143 (1997).